2026 KNS Autumn

Uncertainty Quantification of MIR-PIV Measurements for Pebble-Bed Gap Flow Based on the ISO-GUM Framework

2026.10.29

Seongmin Hong, Jihwan Lim, Sangoh Shin, Hyukjoon Lee, Minseop Song*

Department of Nuclear Engineering, Hanyang University

* hysms@hanyang.ac.kr

CONTENTS

1. Introduction

2. Methods

3. Results and Discussion

4. Conclusions

1. Introduction

Background : Pebble-Bed Reactor

- Pebble-bed reactor (PBR) : high-temperature operation and inherent safety
  - 10^4~10^5 TRISO-fuel pebbles randomly packed in the core
  - Adopted in HTR-PM (China) and KP-FHR (USA)
- Local gap flow governs heat transfer
  - Irregular pore structure → gap-to-gap flow non-uniformity → local hot spots

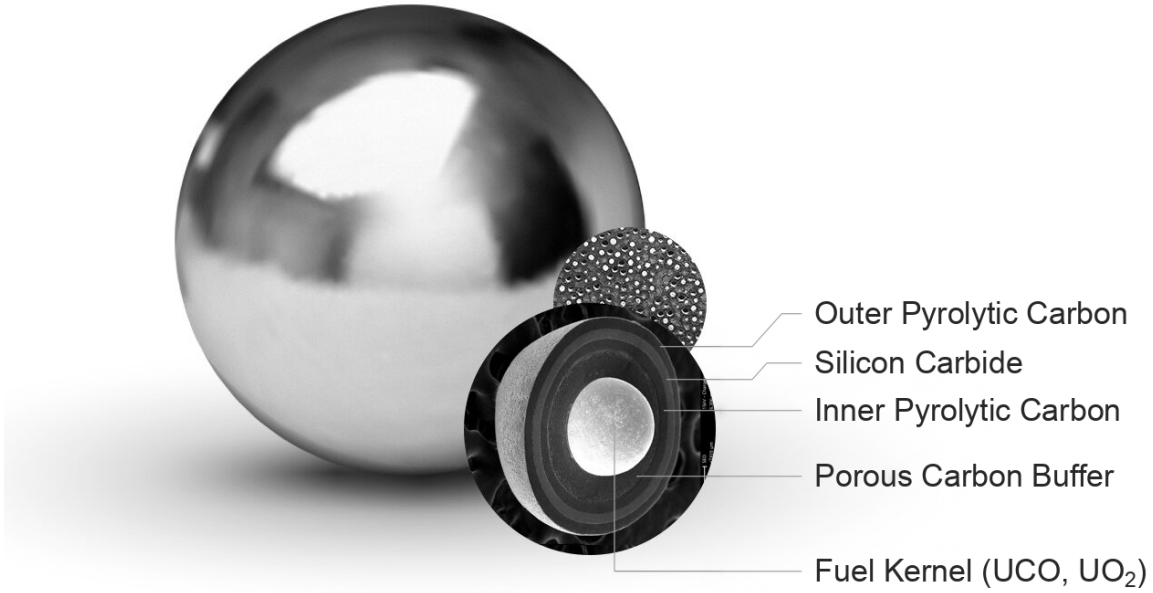


Figure. Shape of Pebble Fuel

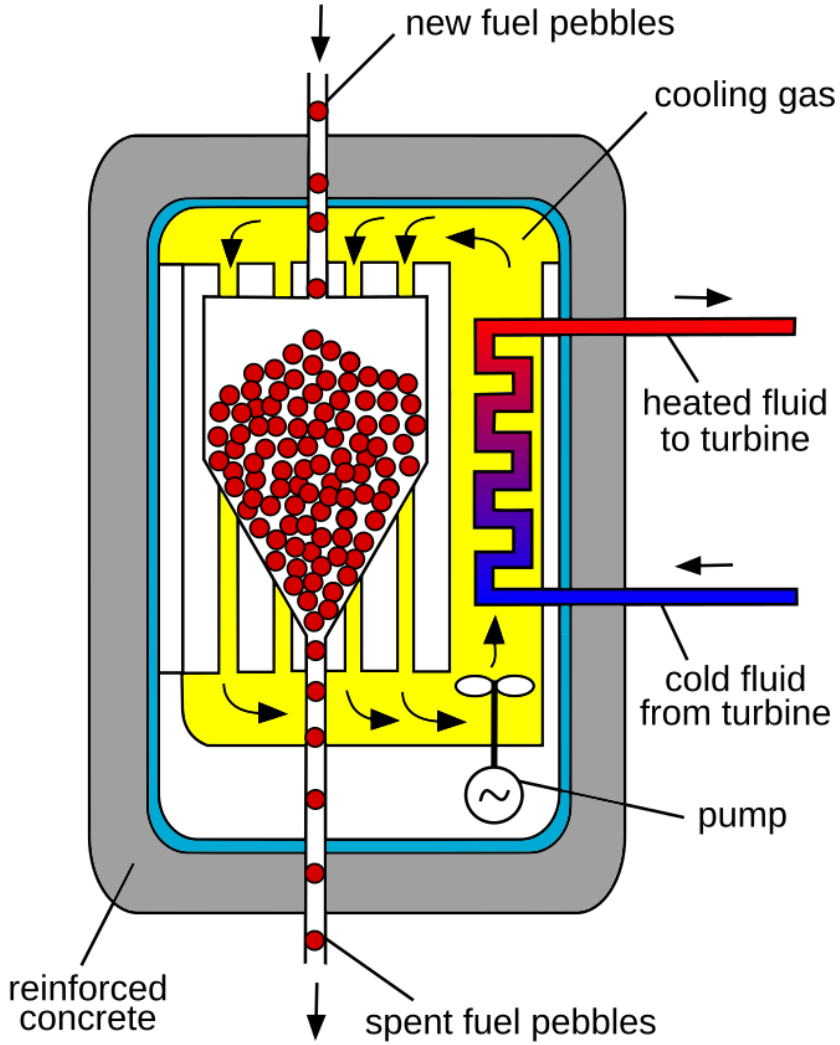


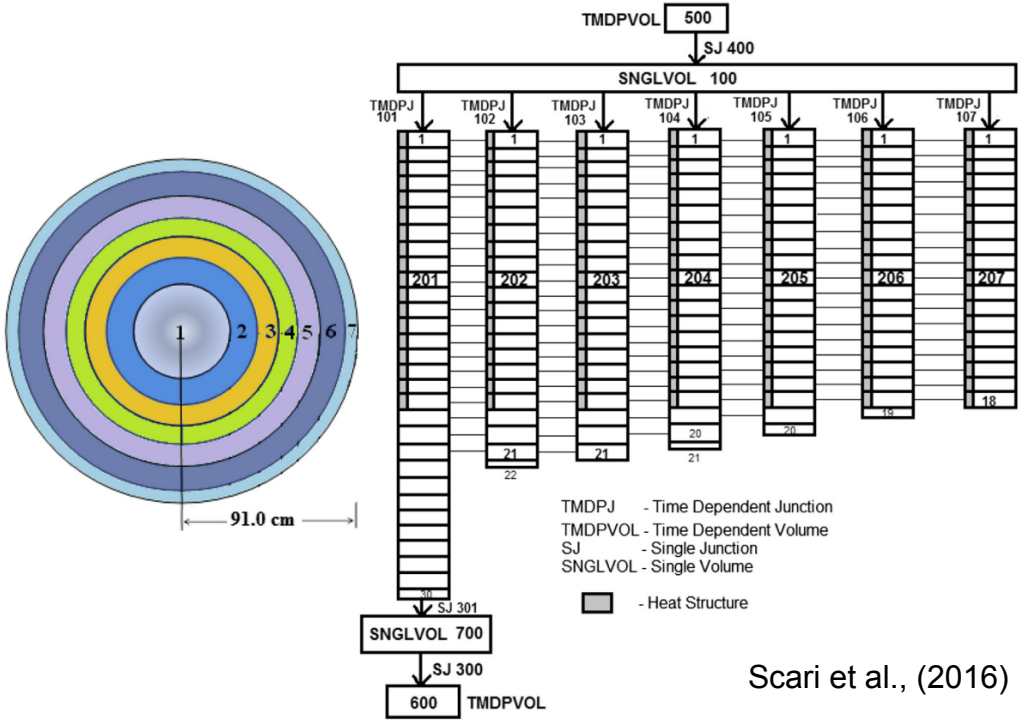
Figure. PBR Schematic Diagram

1. Introduction

Background : Need for Experimental Validation

- Local flow prediction : beyond system codes and porous-media models → CFD
- System codes : validated through an established framework (EMDAP, RG 1.203)
- CFD : no comparable validation framework yet established for nuclear use

System code : region-averaged lumped volumes



Scari et al., (2016)

CFD : locally resolved 3-D mesh

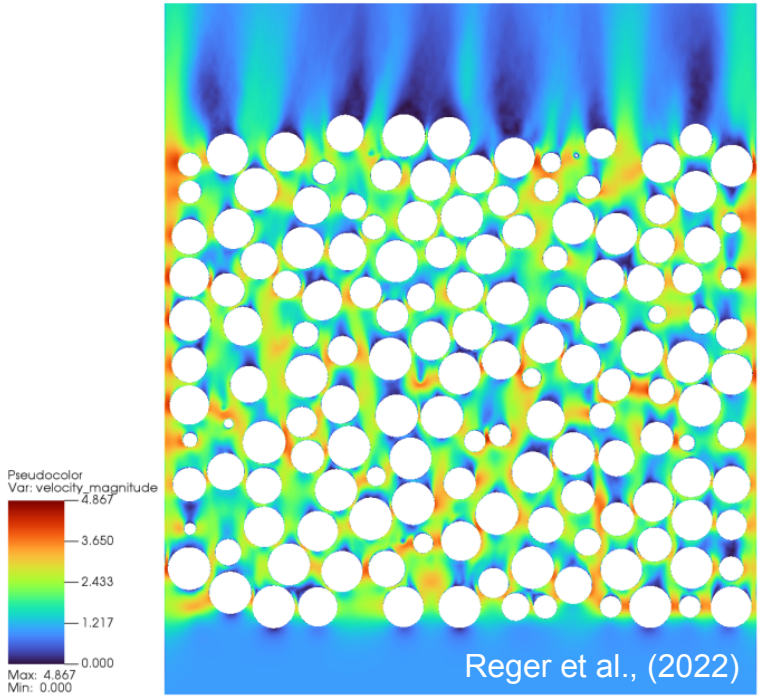


Figure. Pebble bed core analyses : system code (left) vs CFD (right)

Motivation and Objective

- Approach : EMDAP, developed for system codes, applied to pebble-bed CFD
- Gap : assessment base with quantified experimental uncertainty rarely available
- Objective : quantify all MIR-PIV error sources (ISO-GUM) and verify statistical convergence → provide u_D

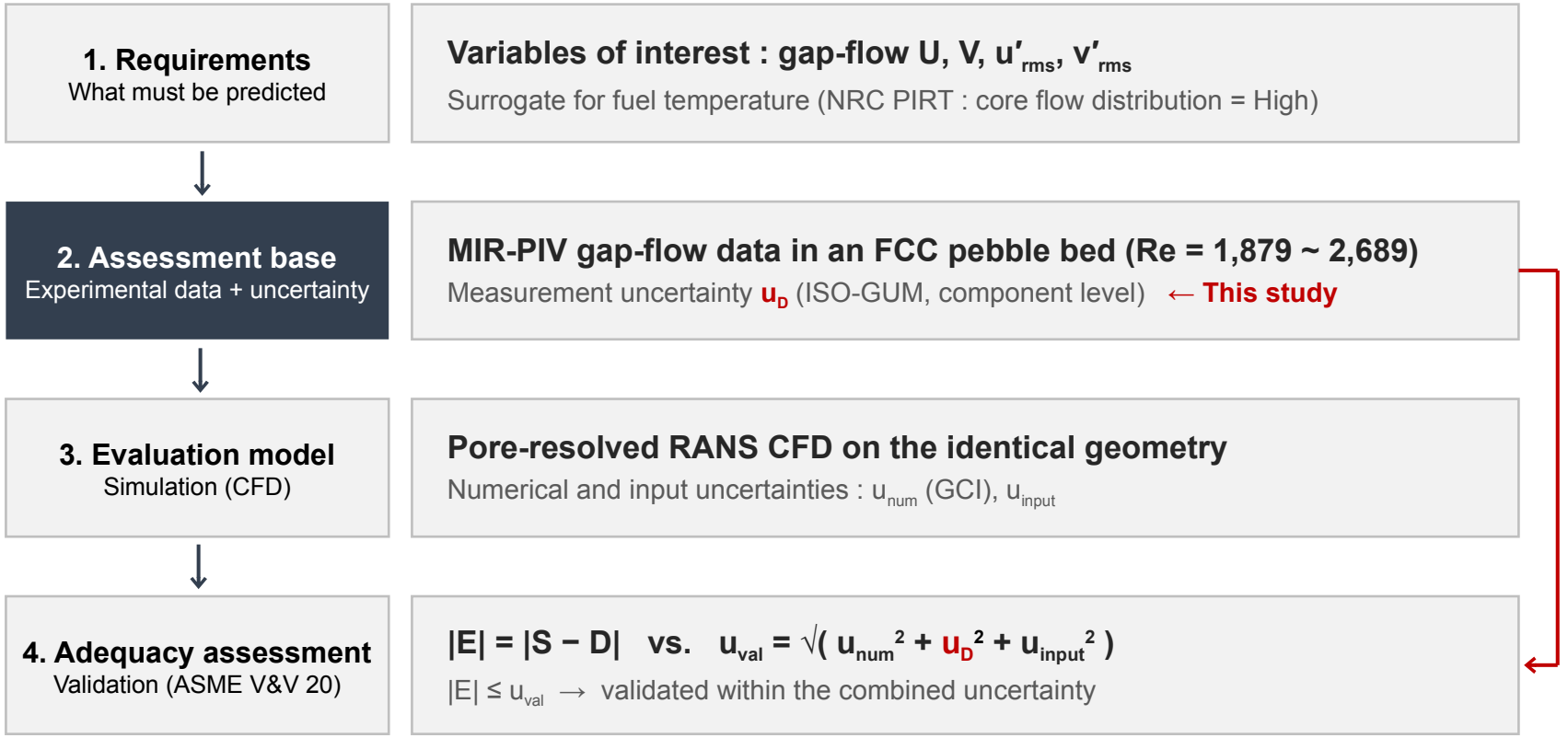


Figure. EMDAP (RG 1.203) and the scope of this study

CONTENTS

1. Introduction

2. **Methods**

3. Results and Discussion

4. Conclusions

2. Methods

Experimental Facility

- Test Loop

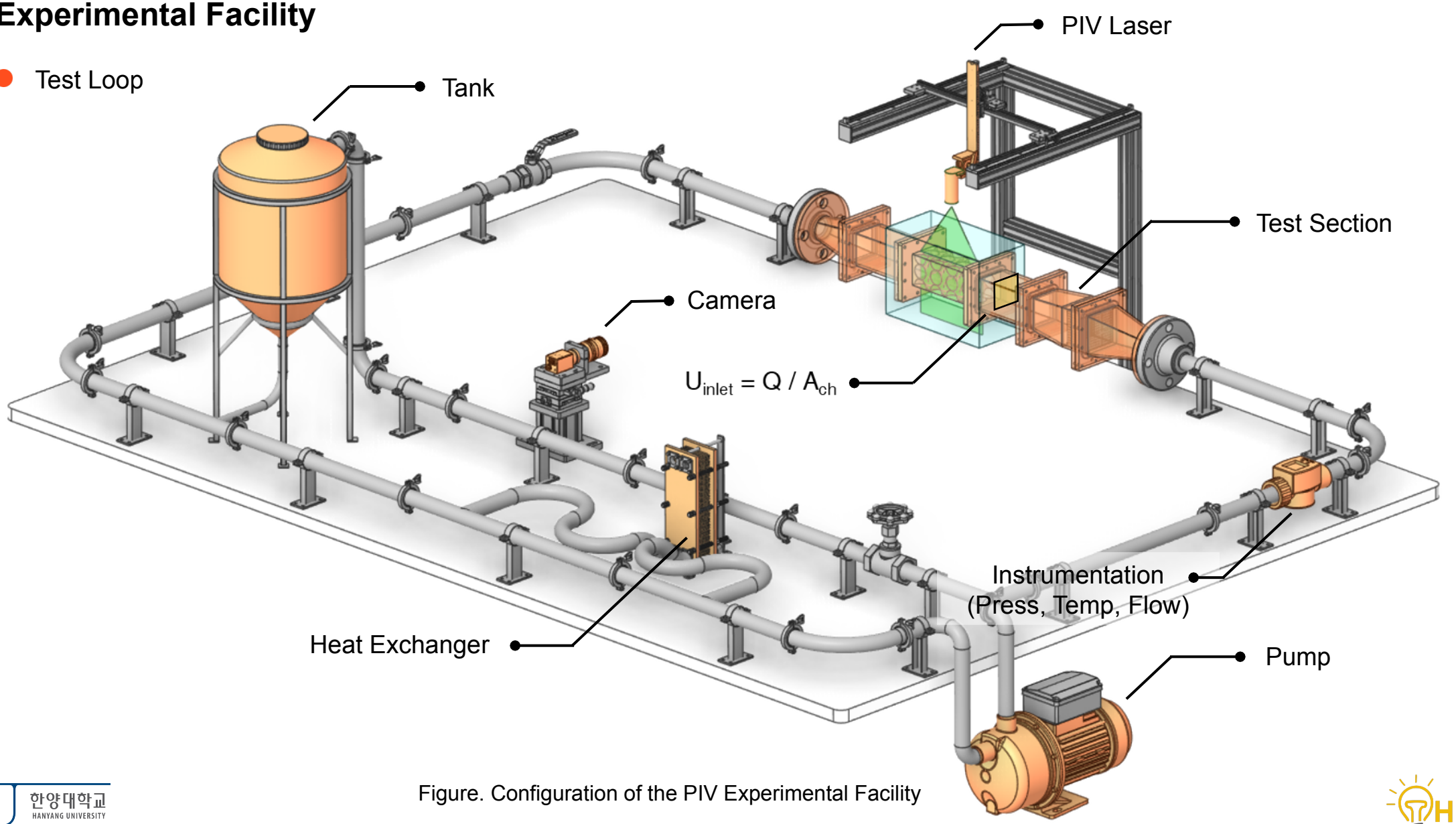


Figure. Configuration of the PIV Experimental Facility

2. Methods

Test Section

- 3D Printed Test Section
  - FCC bed of seven layers (D = 30 mm), outermost pebbles cut at the side walls to form an infinite packing (ε ≈ 0.2595)
  - Honeycomb straightener and flow-development regions of about 5D condition the inlet flow

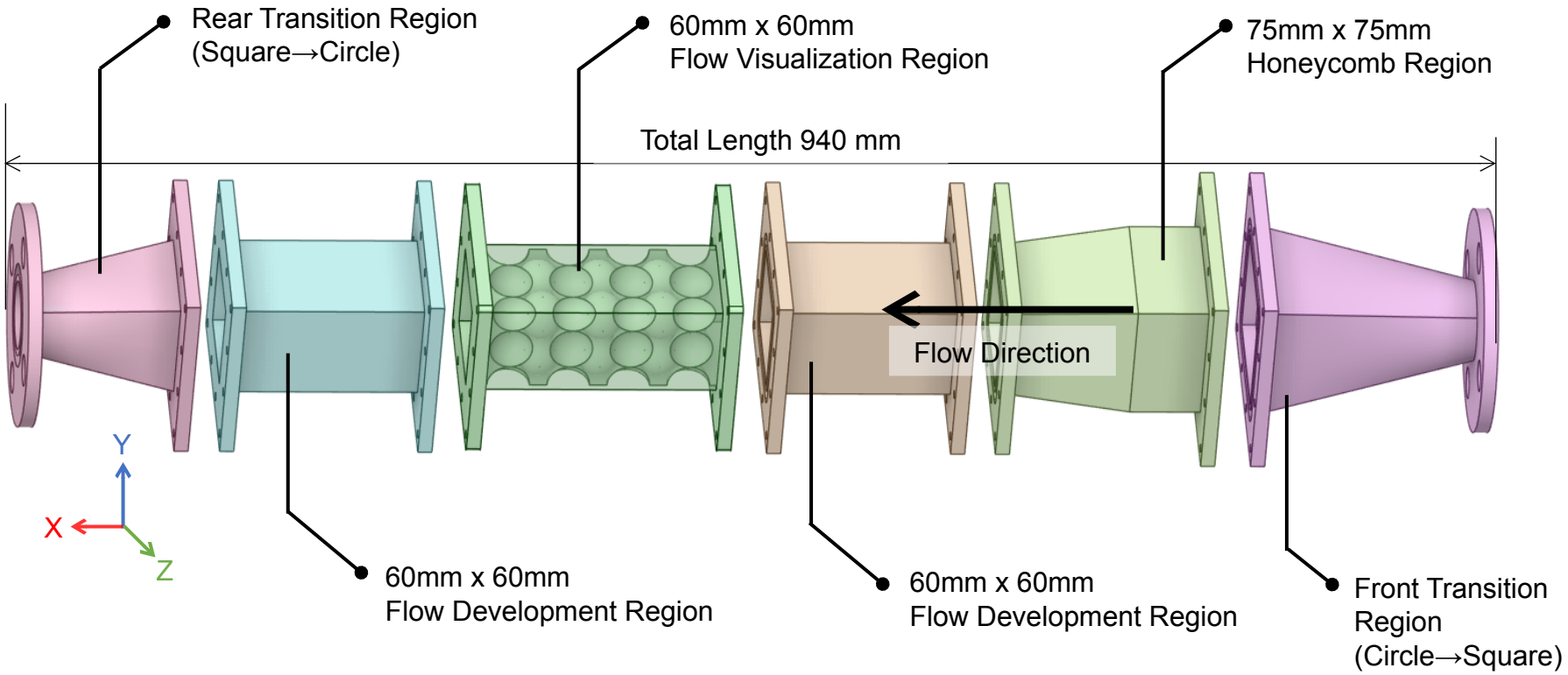


Figure. Configuration of the PIV test section

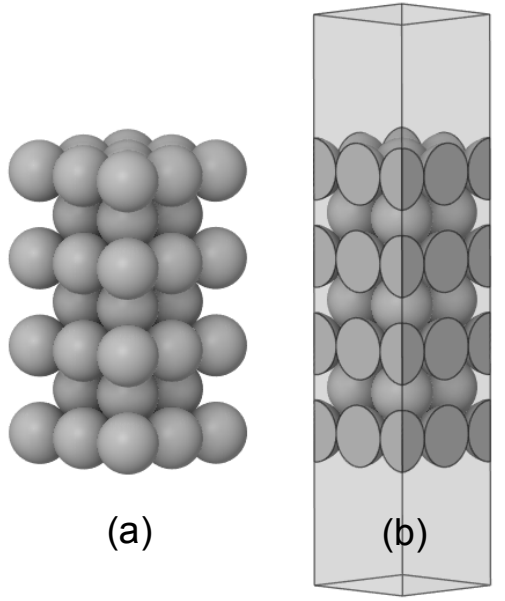
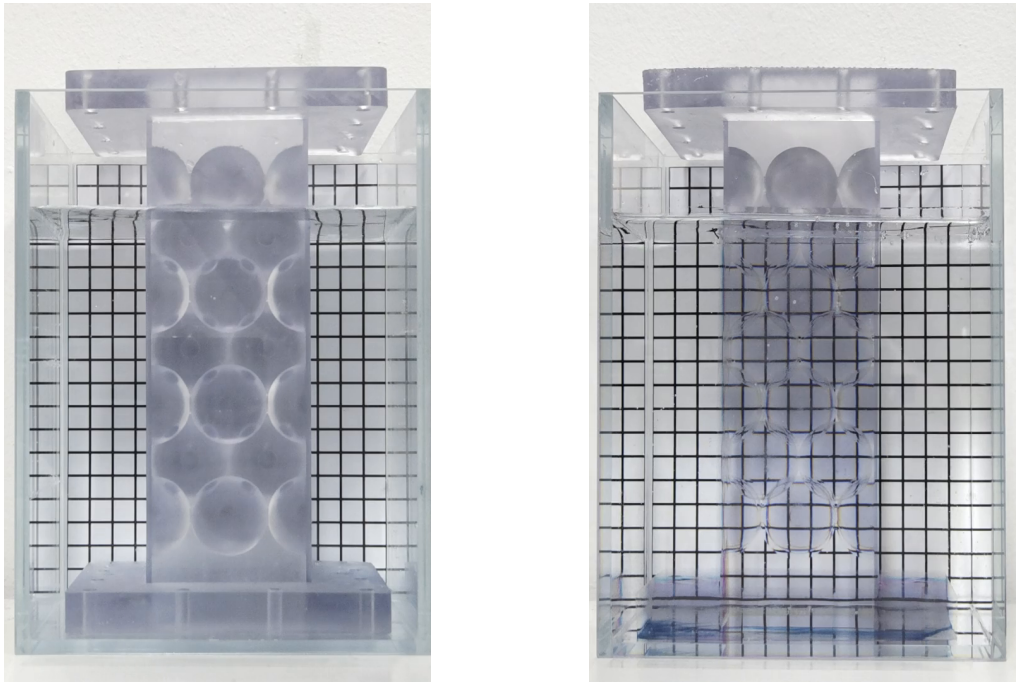


Figure. (a) Schematic of FCC packing (b) FCC domain with wall-truncated outer pebbles.

Matched Index of Refraction Fluid

- Matched index of refraction (MIR) technique
  - Curved pebble surfaces refract light → image distortion
  - MIR : $n_{fluid} = n_{solid} = 1.546$ (84% Benzyl Benzoate + 16% Isopropyl Myristate)
  - Grid test : distortion disappears in the MIR fluid



(a) Water **(b) MIR fluid (n = 1.546)**

Figure. Background-grid test while inserting the 3D-printed pebble bed : (a) water, (b) MIR fluid

2. Methods

PIV Experimental Setup

- Machine and Experiment Conditions Setting
  - *Re* = 1,879 – 2,689 by flow rate (HTR-10 core : *Re* ≈ 2,000)

$$Re = \rho U_{inlet} D / \mu$$

D = 30 mm, $U_{inlet} = Q / A_{ch}$

Table. PIV Machine Setting

Parameter	Value
Laser Power	100%
Laser frequency	10 Hz
Camera Exposure Time	0.2 ms
Straddle Time	50 ~ 75 μs
Captured PIV Image	250 pairs
Interrogation Window	64 × 64 px (50% overlap)

Table. PIV Experiment Conditions

Parameter	Case 1	Case 2	Case 3
Flow Rate	83 L/min	94 L/min	105 L/min
Inlet Velocity	0.3889 m/s	0.4352 m/s	0.4861 m/s
Fluid Temperature	29°C	33°C	37°C
Viscosity	0.006585 Pa•s	0.006137 Pa•s	0.005730 Pa•s
Density	1060.2 kg/m^3	1058.4 kg/m^3	1056.5 kg/m^3
Reynolds Number	1,879	2,252	2,689

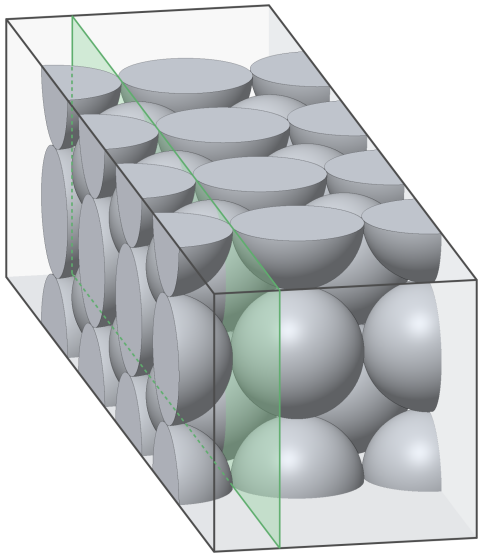


Figure. Measurement Plane

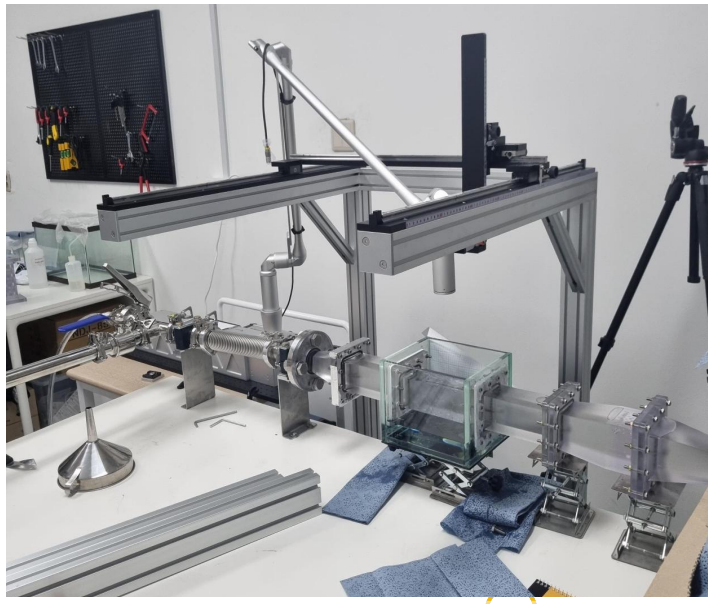


Figure. Flow Visualization Loop Setup

2. Methods

PIV Measurement

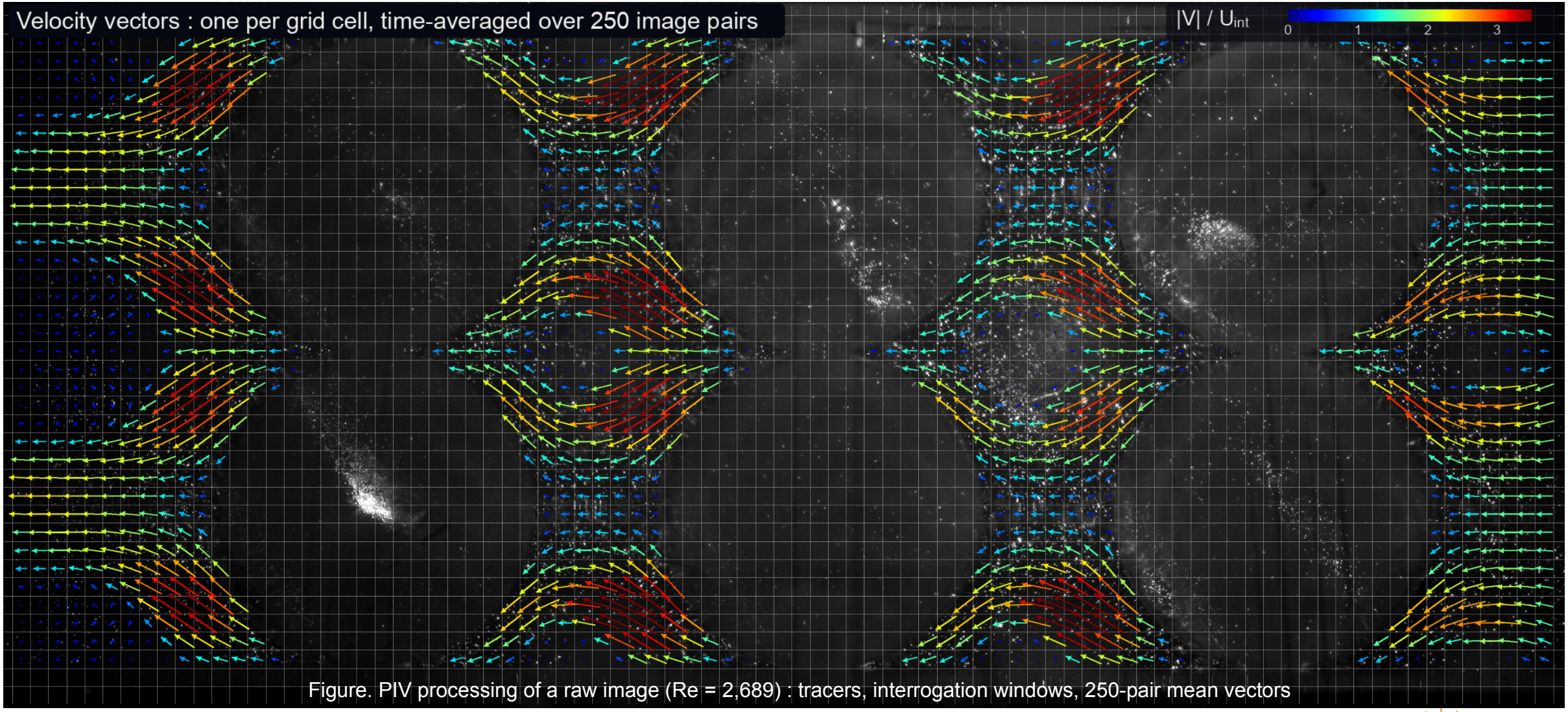


Figure. PIV processing of a raw image (Re = 2,689) : tracers, interrogation windows, 250-pair mean vectors

Uncertainty Quantification Method

- Error sources classified after Sciacchitano (2019) and propagated by the ISO-GUM through U = M·ΔX / Δt

$$u_c = \sqrt{\left[u_{cali}^2 + u_{timing}^2 + u_{slip}^2 + u_{pl}^2 + u_{grad}^2\right] + \left[\frac{\sigma_U}{\sqrt{N}}\right]^2}$$

Combined uncertainty | System uncertainty | Random uncertainty

$$u_e = 1.96 \cdot u_c$$

Expanded uncertainty

	Parameter	Description	Type	Source (ISO-GUM)
Section 2.1. Errors caused by system components	Calibration	Precision of pixel-to-millimeter(mm/px) conversion	Systematic	M
	Timing and synchronization	Laser-pulse and delay-generator timing accuracy	Systematic	Δt
	Particle tracing capability	Particle slip estimated from the Stokes number	Systematic	ΔX
	Peak locking	Bias toward integer-pixel displacement, quantified from the sub-pixel displacement histogram	Systematic	ΔX
	Illumination	Misalignment or intensity-profile mismatch of the two laser pulses, causing variation of individual particle-image intensity	Random	ΔX
Section 2.2 Errors due to the flow	In-plane velocity gradient	Velocity variation within an interrogation window → correlation peak smearing	Systematic	ΔX
	Flow property variation	Run-time fluctuation of fluid properties (ρ, T, μ, Re)	Random	ΔX
	Out of plane motion	Tracer loss across the light sheet (particles exiting / entering during Δt)	Random	ΔX
Section 2.3 Errors due to evaluation technique	PIV software calculation algorithm	Cross-correlation scheme, IW size, window deformation, and outlier validation (Microvec default)	Random	ΔX

CONTENTS

1. Introduction

2. Methods

3. **Results and Discussion**

4. Conclusions

3. Results and Discussion

Measured Mean Velocity Field (Re = 2,689)

- Gap jets accelerate to several times U_{int}, with low-velocity regions behind the pebbles
- Profile along line P with u_e (95%) error bars: reference for profile-level CFD validation

$$U_{inlet} = Q / A_{ch}$$

Superficial inlet velocity (A_{ch} = 60 × 60 mm²)

$$U_{int} = U_{inlet} / \varepsilon$$

Interstitial velocity (FCC, $\varepsilon \approx 0.2595$) → 1.87 m/s at Re = 2,689

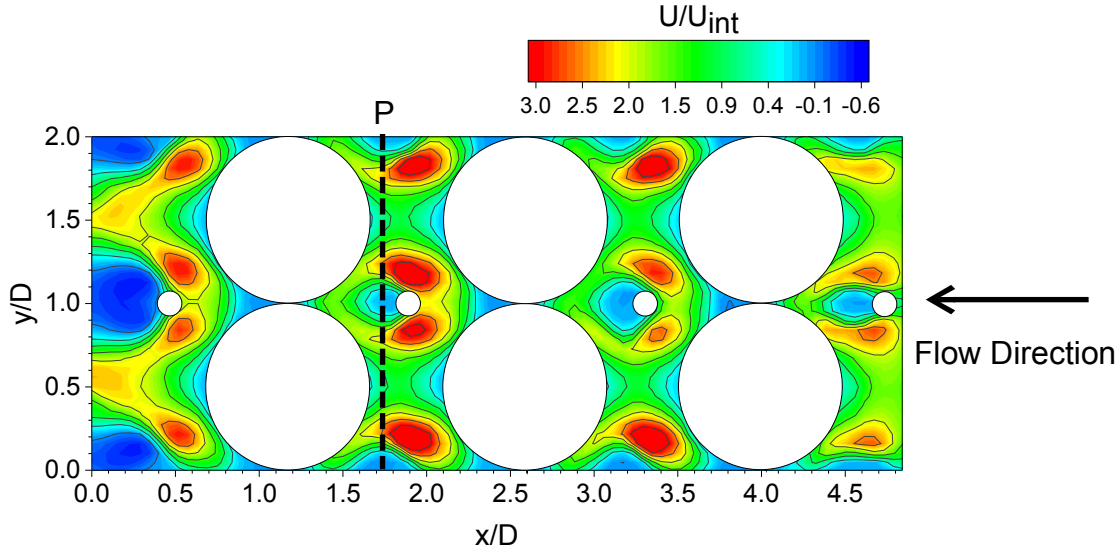


Figure. U/U_{int} contour with profile line P

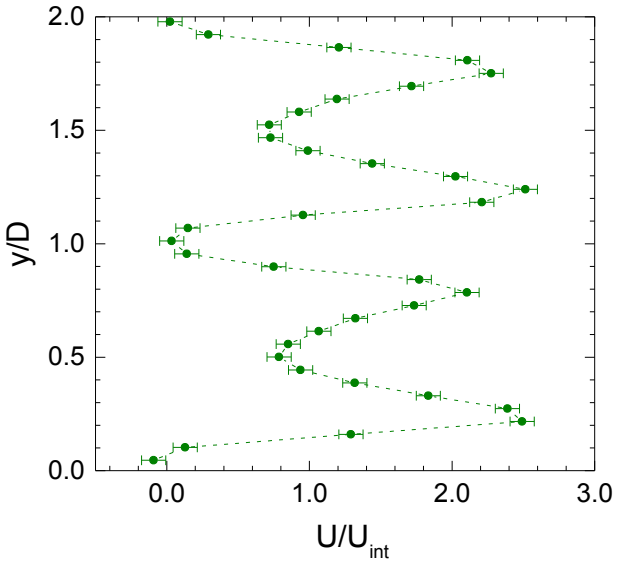


Figure. U/U_{int} along P with u_e (95%) error bars

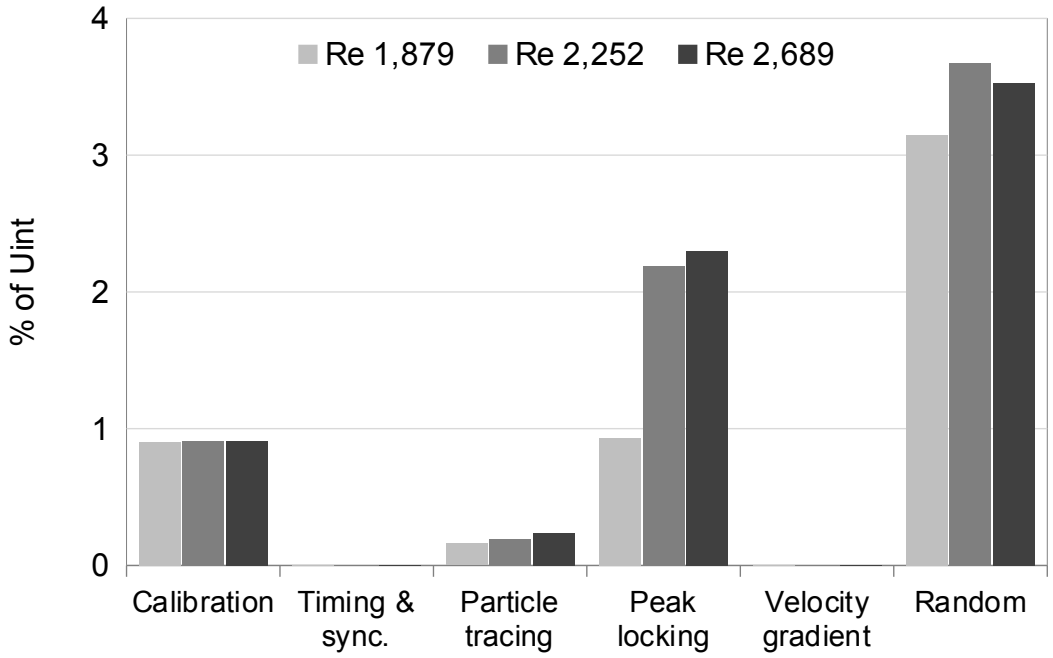
Uncertainty Budget (U, % of U_{int})

- Expanded uncertainty: U 6.7–8.6%, V 5.3–6.8%
  - Higher than typical PIV uncertainty (1–5%) : driven by strong gap-flow turbulence, not by measurement deficiency

Table. Uncertainty budget of U (% of U_{int})

Parameter	Type	Re 1,879	Re 2,252	Re 2,689
Calibration	Systematic	0.90%	0.91%	0.91%
Timing & Synchronization	Systematic	< 0.01%	< 0.01%	< 0.01%
Particle tracing	Systematic	0.16%	0.19%	0.24%
Peak locking	Systematic	0.93%	2.19%	2.30%
In-plane velocity gradient	Systematic	negligible	negligible	negligible
Random	Random	3.15%	3.67%	3.53%
Combined uncertainty (u_c)	-	3.42%	4.38%	4.32%
Expanded uncertainty (u_e)	-	6.69%	8.58%	8.47%

Figure. Standard Uncertainty of each component (% of U_{int})



3. Results and Discussion

Component-Level Uncertainty Analysis

$$u_c = \sqrt{[u_{cali}^2 + u_{timing}^2 + u_{slip}^2 + u_{pl}^2 + u_{grad}^2] + [\frac{\sigma_U}{\sqrt{N}}]^2}$$

- Calibration uncertainty
  - Representative Case : Re 2,689
    - $M = \frac{W}{N_{mask}} = \frac{60mm}{1{,}126\ px} = 0.053286\ mm/px$
  - Form4L printing tolerance (u_W) = ± 0.2% at 60 mm → 0.12 mm
    - $\frac{u_W}{W} = \frac{0.12}{60} = 2 \times 10^{-3}$
  - Mask detection precision (u_N) = ± 10 px
    - $\frac{u_N}{N} = \frac{10}{1126} = 8.88 \times 10^{-3}$
  - Combined Calibration uncertainty (u_M)
    - $(\frac{u_M}{M})^2 = \left(\frac{u_W}{W}\right)^2 + \left(\frac{u_N}{N}\right)^2 \rightarrow u_M = 4.85 \times 10^{-4}\ mm/px$
  - $c_M = \frac{U_{int}^*}{M} = \frac{1{,}873\ mm/s}{0.053286\ mm/px} = 35{,}150\ \frac{px}{s}$
  - $u_{cali} = c_M u_M = 17.05\ mm/s$ (0.91 % of U_{int})

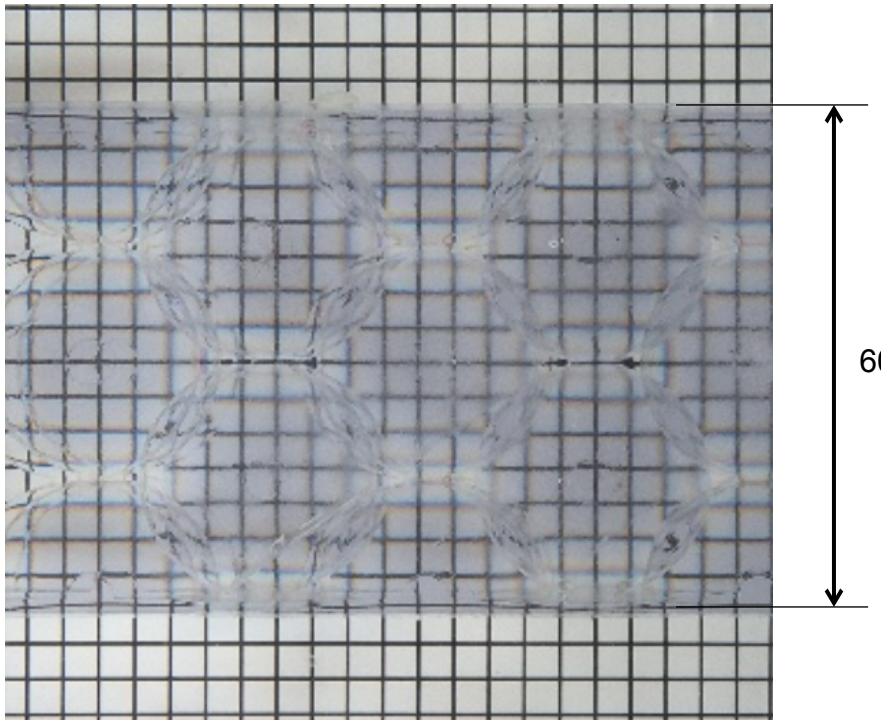


Figure. In-situ calibration : channel width (W_{ch} = 60mm) in the measurement plane as the reference length

* U_{int} : Interstitial velocity, $U_{superficial}/\varepsilon$

3. Results and Discussion

Component-Level Uncertainty Analysis

$$u_c = \sqrt{[u_{cali}^2 + u_{timing}^2 + u_{slip}^2 + u_{pl}^2 + u_{grad}^2] + [\frac{\sigma_U}{\sqrt{N}}]^2}$$

- Timing and synchronization uncertainty (u_{timing})
  - Laser timing jitter ($u_{\Delta t,laser}$) $< 0.5\ ns$
    - $\frac{u_{\Delta t,laser}}{\Delta t} = \frac{0.5\ ns}{50\ \mu s} = 1.0\times10^{-5}$
  - Synchronizer RMS jitter ($u_{\Delta t,sync}$) $\leq 50\ ps$
    - $\frac{u_{\Delta t,DG}}{\Delta t} = \frac{50\ ps}{50\ \mu s} = 1.0\times10^{-6}$
  - Combined timing uncertainty ($u_{\Delta t}$)
    - $(\frac{u_{\Delta t}}{\Delta t})^2 = \left(\frac{u_{\Delta t,laser}}{\Delta t}\right)^2 + \left(\frac{u_{\Delta t,sync}}{\Delta t}\right)^2 \rightarrow u_{\Delta t} \approx 0.5\ ns$
  - $c_{\Delta t} = \frac{U_{int}}{\Delta t} = \frac{1{,}873\ mm/s}{50\ \mu s} = 3.75\times10^7\ mm/s^2$
  - $u_{timing} = c_{\Delta t} u_{\Delta t} = 1.88\times10^{-2} mm/s$ (< 0.01 % of U_{int})

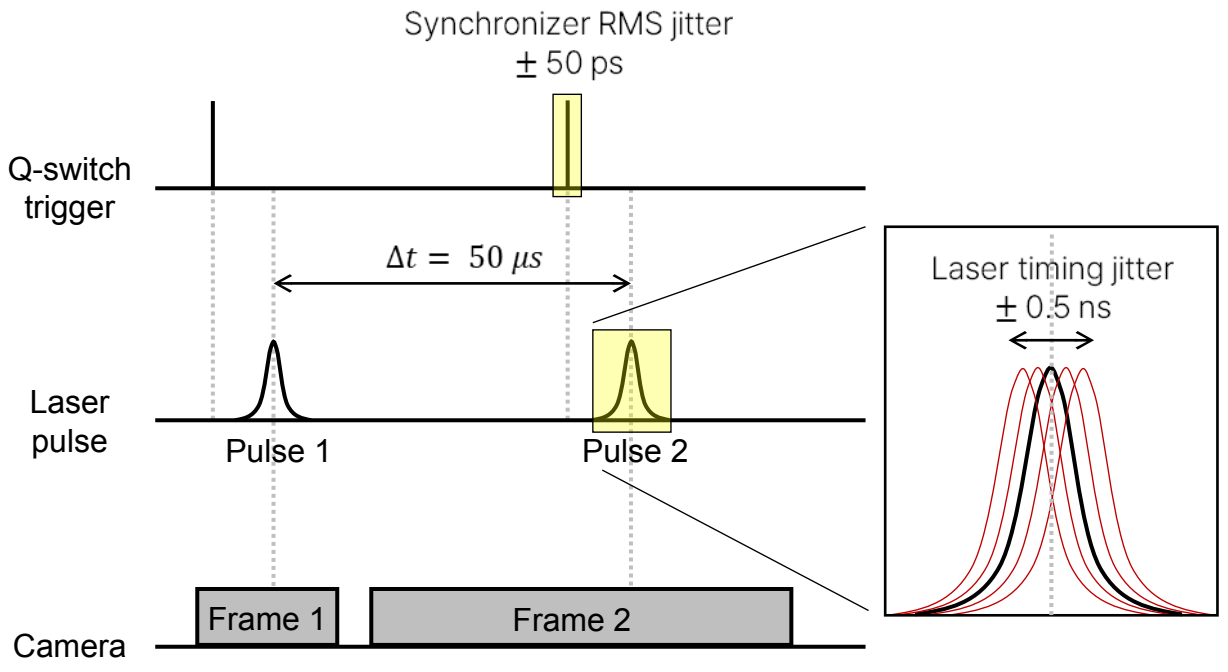


Figure. PIV timing sequence and timing jitter

Component-Level Uncertainty Analysis

$$u_c = \sqrt{[u_{cali}^2 + u_{timing}^2 + u_{slip}^2 + u_{pl}^2 + u_{grad}^2] + [\frac{\sigma_U}{\sqrt{N}}]^2}$$

- Particle tracing capability uncertainty (u_{slip})
  - Seeding particle property
    - Diameter (D_p) = 15μm
    - Density (ρ_p) = 1,100 kg/m³
  - Stokes number
    - $Stk \equiv \frac{\tau_p}{\tau_f} = \frac{D_p^2 \times \rho_p}{18\mu_f} \times \frac{U_{max}}{D} = \frac{(15\times10^{-6})^2 \times 1100}{18\times(5.73\times10^{-3})} \times \frac{7.5}{30\times10^{-3}}$
      $\approx 6.0\times10^{-4}$
  - $u_{slip} \equiv \tau_p \times a \approx Stk \times U_{max} = 6.0\times10^{-4}\times7.5 = 4.5\ mm/s$
    (0.24 % of U_{int})

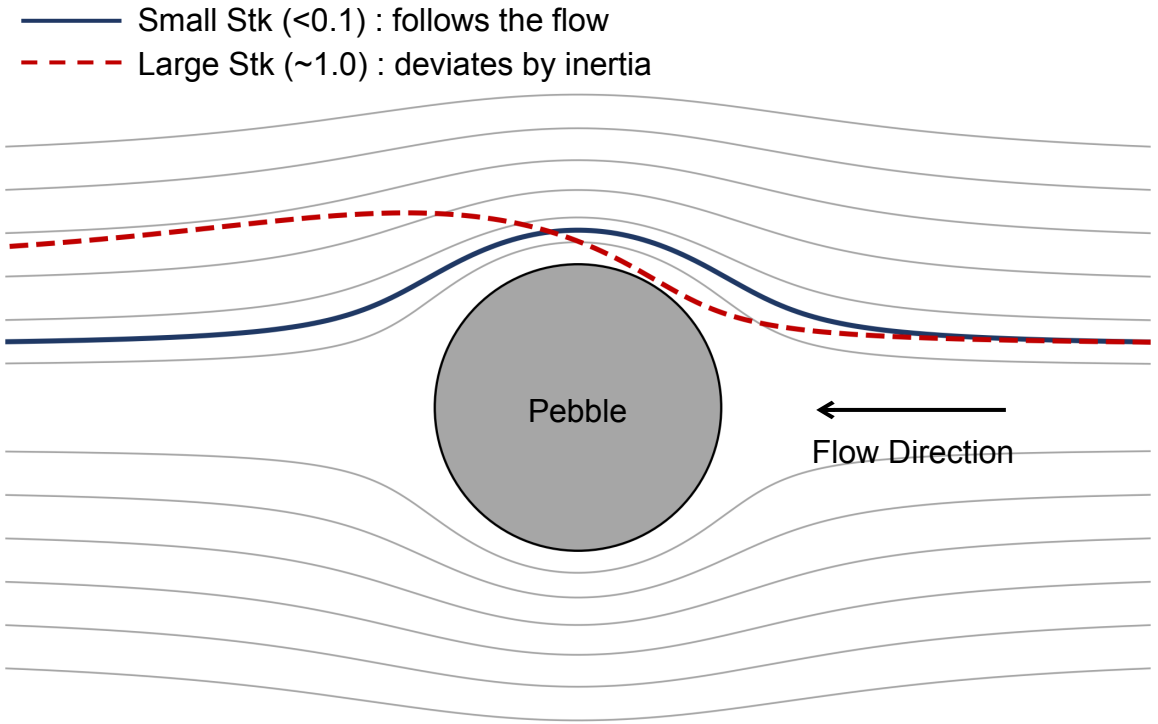


Figure. Particle tracing by Stokes number

3. Results and Discussion

Component-Level Uncertainty Analysis

$$u_c = \sqrt{\left[{u_{cali}}^2 + {u_{timing}}^2 + {u_{slip}}^2 + {u_{pl}}^2 + {u_{grad}}^2\right] + \left[\frac{\sigma_U}{\sqrt{N}}\right]^2}$$

- Peak Locking uncertainty
  - Peak locking
    - Bias toward integer-pixel displacement, quantified from the sub-pixel displacement histogram
    - Caused by the 3-point Gaussian sub-pixel fit on narrow, noisy correlation peaks (particle image < 2 px)
  - Peak locking measurement
    - $f(\psi) = 1 + 2\pi C \cdot \cos(2\pi\psi)\,, \quad C = 0.0572\ px$
  - Bias : [measure – true]
    - $B(\psi) = -C \cdot \sin(2\pi\psi)$
  - $u_{\Delta X} = RMS[B(\psi)] = \frac{C}{\sqrt{2}} = \frac{0.0572}{\sqrt{2}} = 0.0404\ px$
  - $c_{\Delta X} = \frac{M}{\Delta t} = \frac{0.053286\ mm/px}{50\ \mu s} = 1.07\times10^3 mm/px \cdot s$
  - $u_{pl} = c_{\Delta X} u_{\Delta X} = 43.1\ mm/s$ (2.30 % of U_{int})

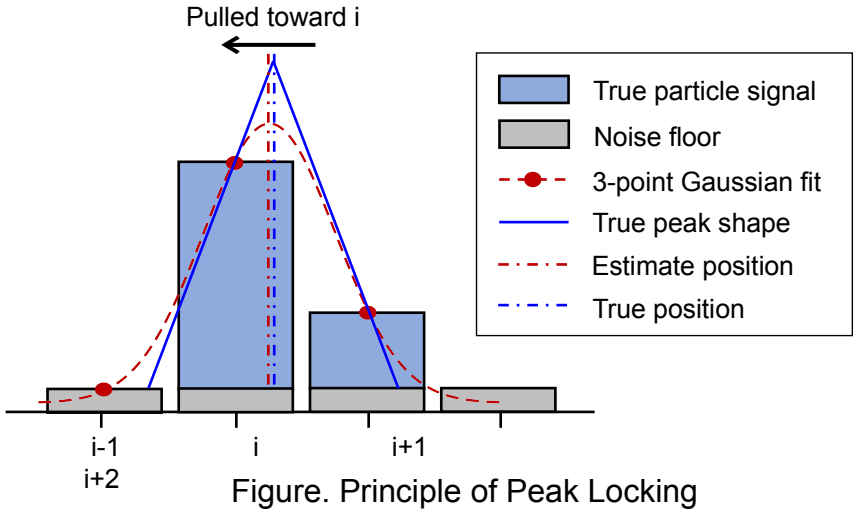


Figure. Principle of Peak Locking (3-point Gaussian fit)

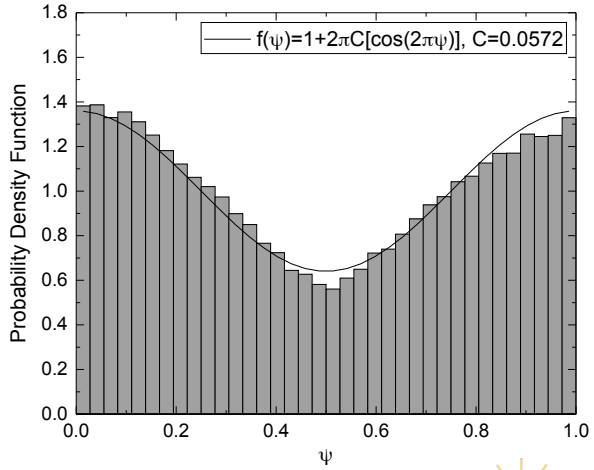


Figure. Histogram of sub-pixel particle displacement ψ at Re=2,689

3. Results and Discussion

Component-Level Uncertainty Analysis

$$u_c = \sqrt{[u_{cali}^2 + u_{timing}^2 + u_{slip}^2 + u_{pl}^2 + u_{grad}^2] + [\frac{\sigma_U}{\sqrt{N}}]^2}$$

- In-plane velocity gradient uncertainty
  - Cause : velocity gradient within a window → unequal particle displacement → broadened correlation peak
  - Mitigation : iterative multi-grid window deformation (Scarano & Riethmuller, 2000)
  - Residual error : may remain in narrow gaps → assumed negligible relative to the dominant components (not separately quantified)

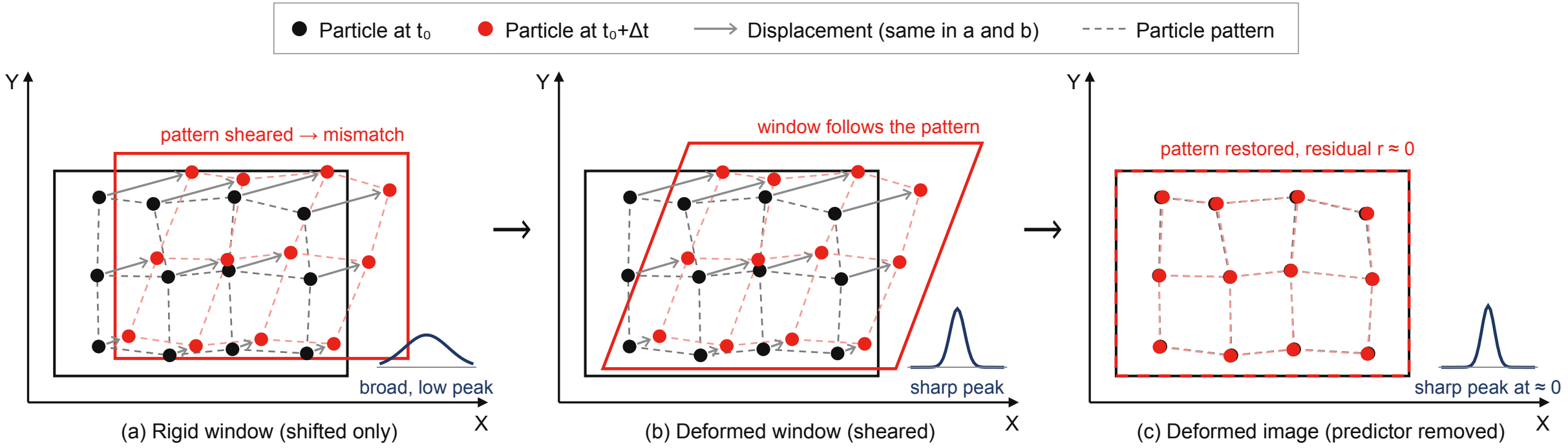


Figure. Window deformation under an in-plane velocity gradient

3. Results and Discussion

Component-Level Uncertainty Analysis

$$u_c = \sqrt{\left[u_{cali}^2 + u_{timing}^2 + u_{slip}^2 + u_{pl}^2 + u_{grad}^2\right] + \left[\frac{\sigma_U}{\sqrt{N}}\right]^2}$$

- Random uncertainty
  - Temporal std. at each grid point (turbulence + random uncertainty)
  - σ_U = 1,047 mm/s
  - N = 250 independent image pairs

  $\frac{\sigma_U}{\sqrt{N}} = 66.2\ mm/s$ (3.53 % of U_{int})

- Statistical convergence (95 % envelope)
  - Mean U, V : converged within N = 250
  - u'_{rms}, v'_{rms} : converge more slowly than the mean velocity

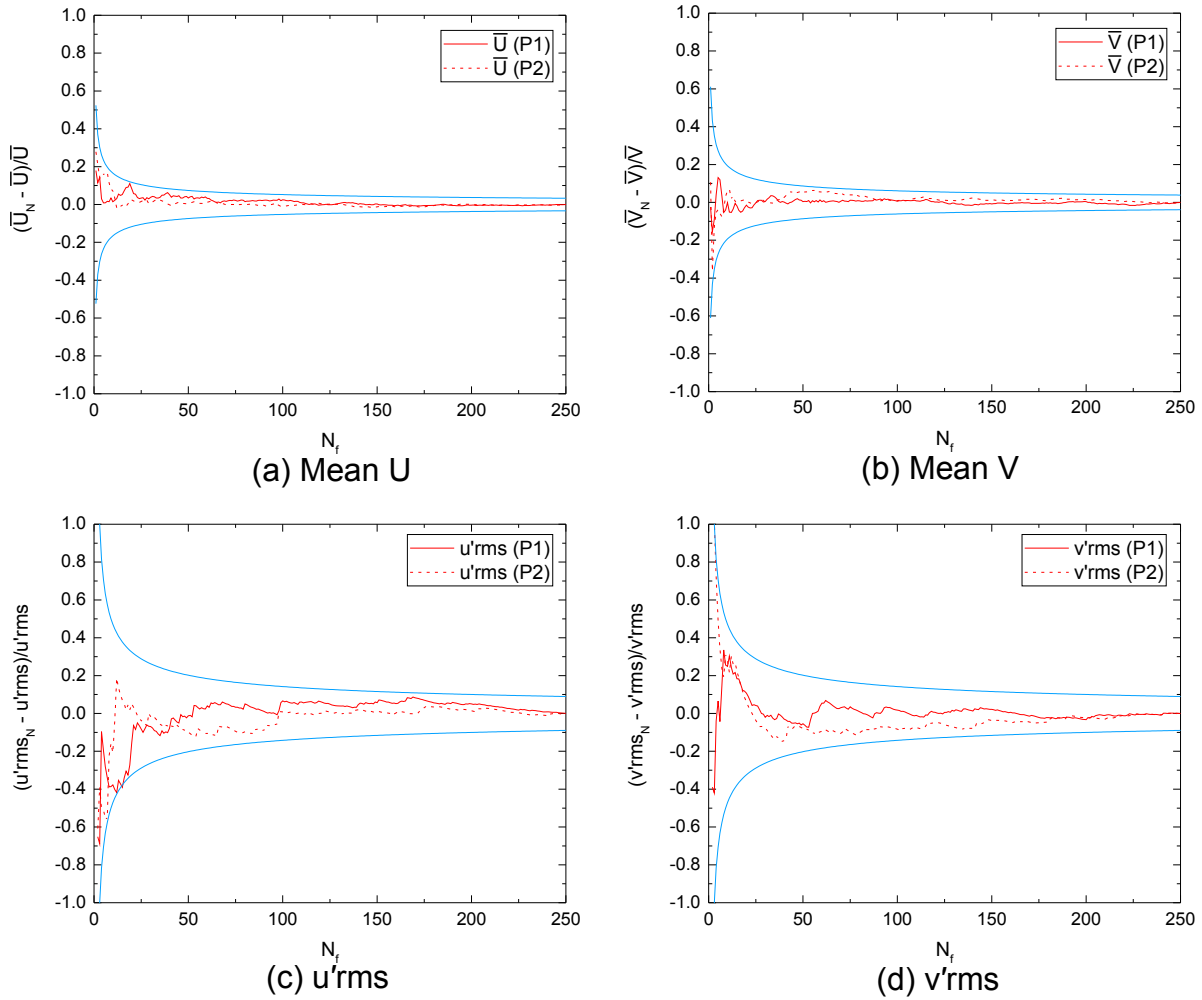


Figure. Convergence histories with 95% envelopes (Re = 2,689)

Application : PIV–CFD Comparison of the Mean Velocity (Re = 2,689)

(a) PIV (measured)

(b) CFD (k-ε Realizable, EWT)

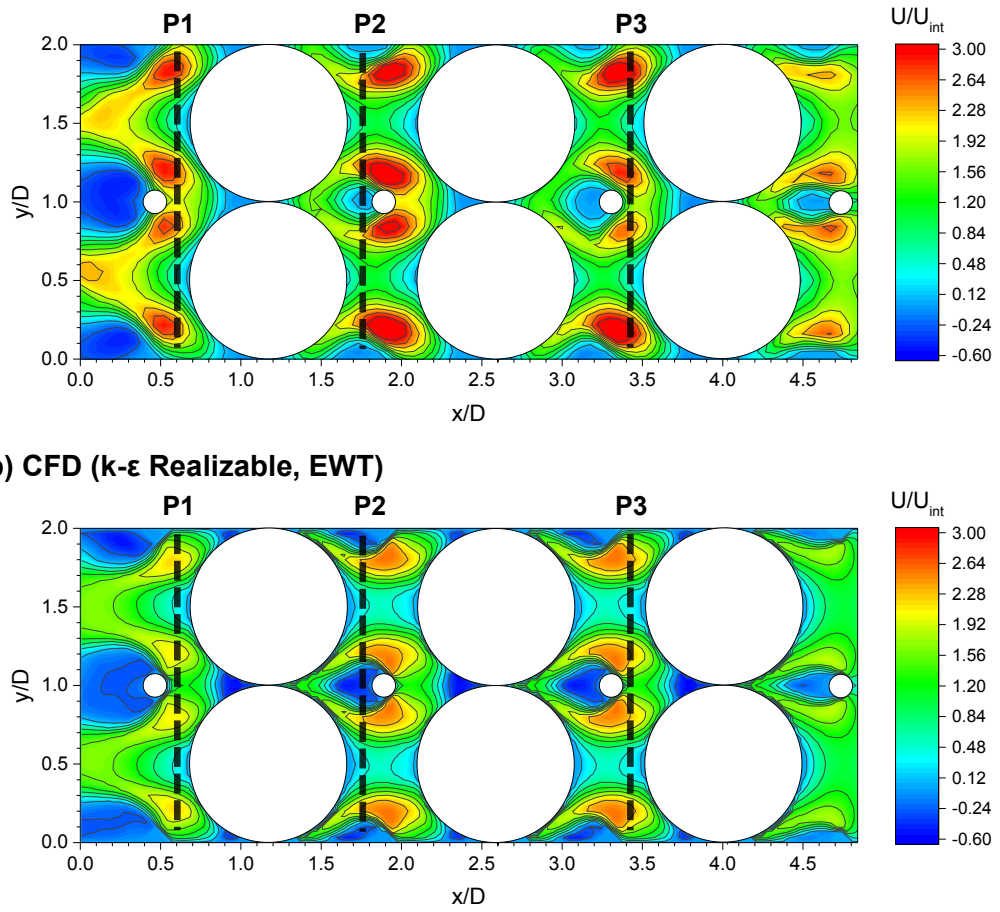


Figure. Mean streamwise velocity : PIV vs. CFD (Re = 2,689)

- Spatial structure of the gap jets reproduced
- Gap-jet peak velocity underpredicted by all RANS models

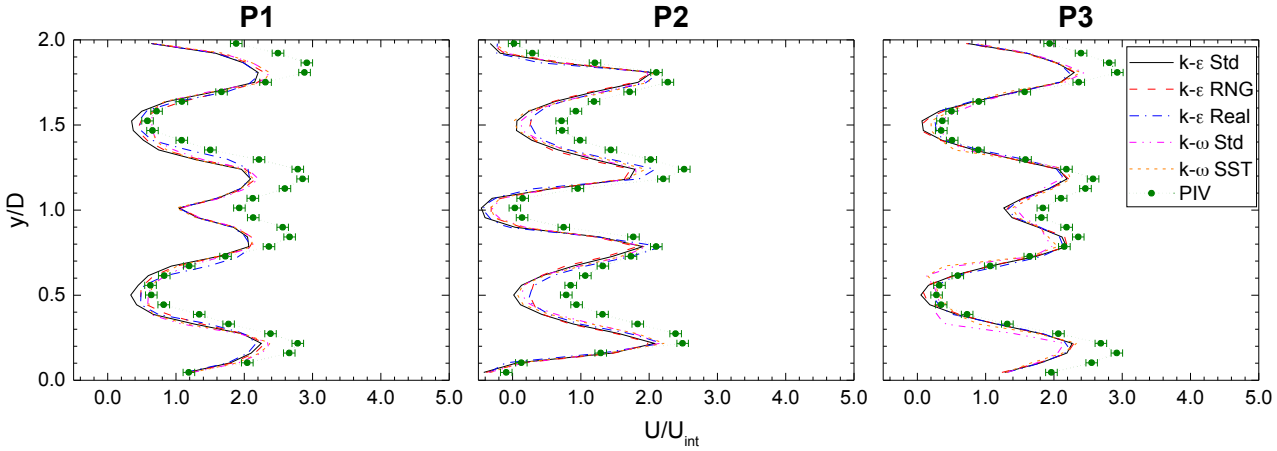


Figure. U / U_{int} profiles : PIV with u_e (95%) error bars vs. five RANS models

Use in ASME V&V 20 and Limitations

- ASME V&V 20 validation criterion
  - Comparison error : $E = S - D$ (simulation − experiment)
  - Validation uncertainty : $u_{val} = \sqrt{(u_{num}^2 + u_{input}^2 + u_D^2)}$
  - $|E| \leq u_{val} \rightarrow$ model validated within the validation uncertainty
- Role of this study
  - $u_D = u_e$: U 6.7~8.6 %, V 5.3~6.8 % of U_{int}
  - u_{num}, u_{input} : evaluated on the CFD side
- Limitations
  - 2D-2C, single plane ($W_{ch}/4$) : in-plane statistics only (W not measured)
  - N = 250 : sufficient for the mean (U, V), limited for turbulence intensity (u'_{rms}, v'_{rms})
  - Residual refractive index mismatch near curved pebble surfaces : not separately quantified

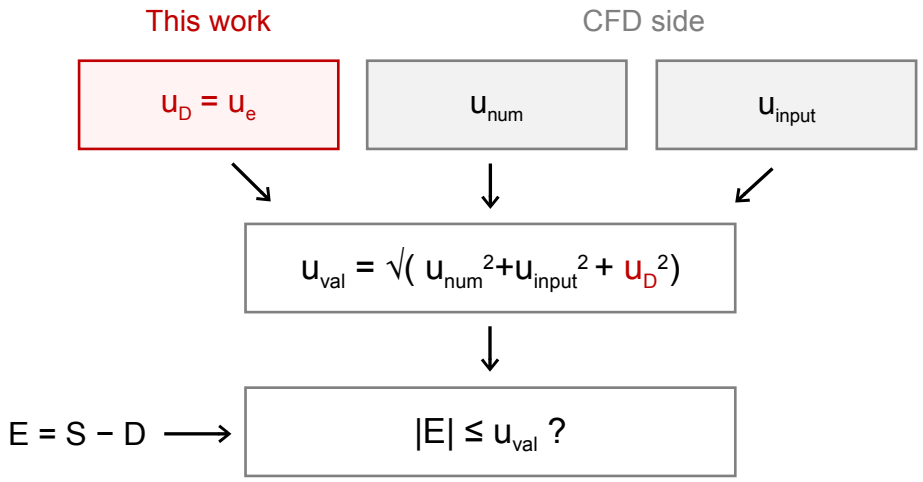


Figure. ASME V&V 20 validation framework

CONTENTS

1. Introduction

2. Methods

3. Results and Discussion

4. Conclusions

4. Conclusions

Summary and Future Work

- An ISO GUM-based uncertainty-quantification procedure for pebble-bed MIR-PIV established
- Uncertainty-quantified dataset obtained → directly usable as u_D in ASME V&V 20

Summary		Future Work
Expanded uncertainty	u_e (95 %) : U 6.7–8.6 %, V 5.3–6.8 % of U_{int}	Quantitative comparison with CFD turbulence models, using u_e as u_D in ASME V&V 20
Random term (largest)	3.2–3.7 % : turbulent gap-flow fluctuation → reducible by sample size N	Larger sample size for converged turbulence statistics
Systematic terms	Peak locking dominant (0.93–2.30 %, condition-dependent → measured per condition), calibration ≈ 0.9 %, others < 0.3 %	
Convergence	Mean converged at N = 250, turbulence intensity carries ≈ 10 % finite-sample uncertainty	Application to other packed structures

Thank you

Seongmin Hong

hsm8807@hanyang.ac.kr

Acknowledgement : This work was supported by the Korea Institute of Energy Technology Evaluation and Planning (KETEP) grant funded by MOTIE (No. RS-2024-00398867) and the National Research Foundation of Korea (NRF) grant funded by MSIT (No. RS-2025-02310831).

Pebble Contact Treatment

- Bridge (d/D = 0.15) adopted : printable as one body, identical geometry in the test section and CFD, minimal porosity change (<1%)

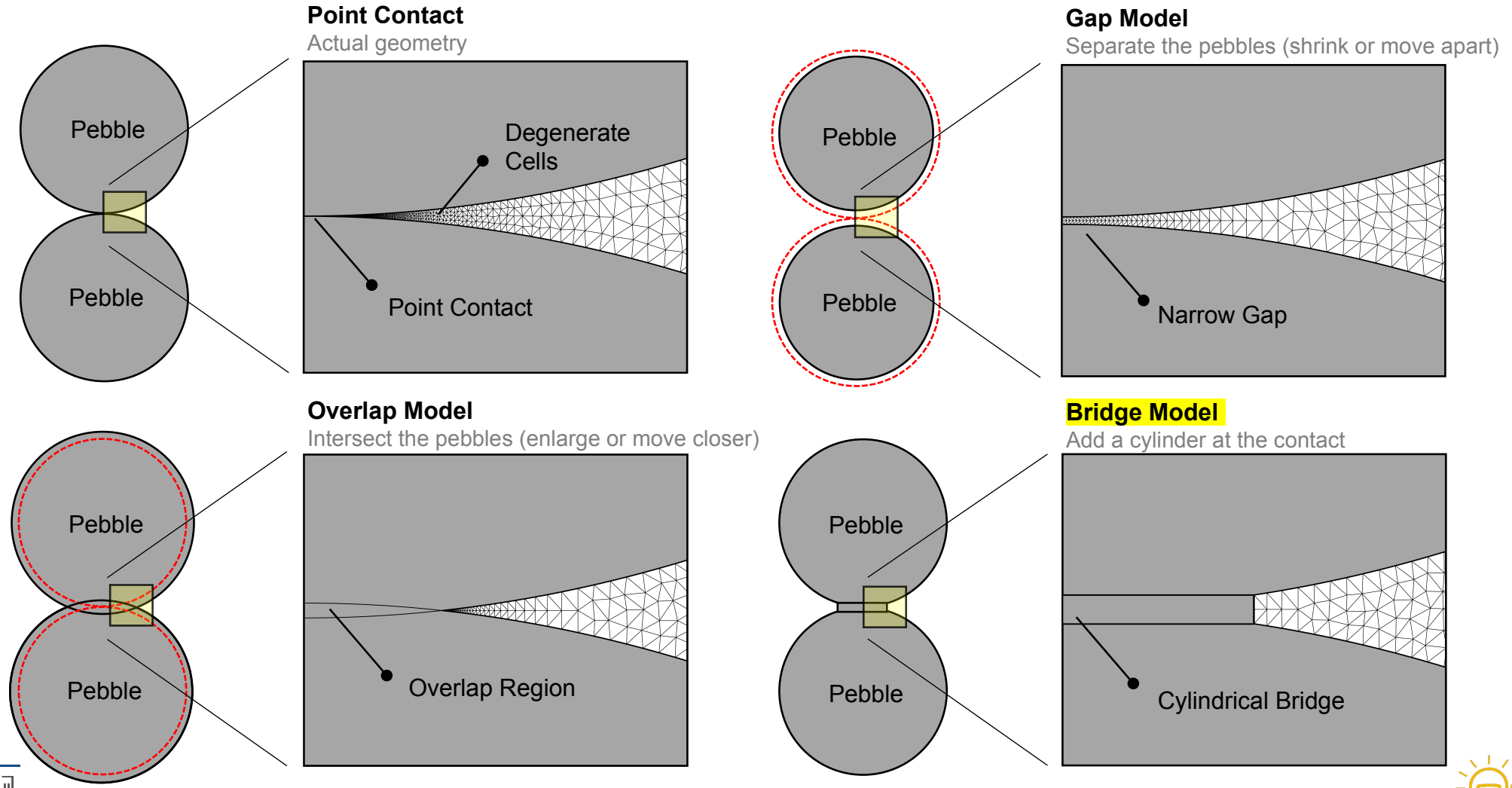


Figure. Mesh near the pebble contact point

Appendix.

Uncertainty Quantification Method : ISO-GUM Propagation

- Uncertainty propagation through the measurement model (input quantities ΔX, Δt, M)
  - The local flow velocity U

$$U = \frac{\Delta x}{\Delta t} = \frac{M \cdot \Delta X}{\Delta t}$$

    - where
      - Δt : time interval between two consecutive PIV frames [s]
      - Δx : physical displacement of tracer particles during Δt [mm]
      - M : magnification factor (spatial calibration), [mm/px]
      - ΔX : pixel displacement of tracer particle images, measured by cross-correlation [px]

  - ISO-GUM uncertainty propagation applied to U = M·ΔX/Δt (independent inputs, products/quotients → sum of squared relative uncertainties).

Relative form : $\left(\frac{u_U}{U}\right)^2 = \left(\frac{u_{\Delta X}}{\Delta X}\right)^2 + \left(\frac{u_{\Delta t}}{\Delta t}\right)^2 + \left(\frac{u_M}{M}\right)^2$ or

Absolute form : $u_U{}^2 = (c_{\Delta X} u_{\Delta X})^2 + (c_{\Delta t} u_{\Delta t})^2 + (c_M u_M)^2$

    - where
      - $c_{\Delta X} \equiv \frac{\partial U}{\partial \Delta X} = \frac{M}{\Delta t} = \frac{U}{\Delta X}$, $c_{\Delta t} \equiv \frac{\partial U}{\partial \Delta t} = -\frac{U}{\Delta t}$, $c_M \equiv \frac{\partial U}{\partial M} = \frac{\Delta X}{\Delta t} = \frac{U}{M}$